SANDIA REPORT

SAND2014-18565
Unlimited Release
Printed October 2014

Hierarchical Multiscale Method Development for Peridynamics

Stewart A. Silling
James V. Cox

Prepared by
Sandia National Laboratories
Albuquerque, New Mexico 87185 and Livermore, California 94550

Sandia National Laboratories is a multi-program laboratory managed and operated by Sandia Corporation, a wholly owned subsidiary of Lockheed Martin Corporation, for the U.S. Department of Energy's National Nuclear Security Administration under contract DE-AC04-94AL85000.

Sandia National Laboratories

Issued by Sandia National Laboratories, operated for the United States Department of Energy by Sandia Corporation.

Available to DOE and DOE contractors from
U.S. Department of Energy
Office of Scientific and Technical Information
P.O. Box 62
Oak Ridge, TN 37831

Telephone: (865) 576-8401
Facsimile: (865) 576-5728
E-Mail: reports@adonis.osti.gov
Online ordering: http://www.osti.gov/bridge

Available to the public from
U.S. Department of Commerce
National Technical Information Service
5285 Port Royal Rd
Springfield, VA 22161

Telephone: (800) 553-6847
Facsimile: (703) 605-6900
E-Mail: orders@ntis.fedworld.gov
Online ordering: http://www.ntis.gov/help/ordermethods.asp?loc=7-4-0#online

SAND2014-18565
Unlimited Release
Printed October 2014

Hierarchical Multiscale Method Development for Peridynamics

Stewart A. Silling
Multiscale Science Department
Sandia National Laboratories
P.O Box 5800
Albuquerque, NM 87185-1322

James V. Cox
Solid Mechanics Department
Sandia National Laboratories
P.O. Box 5800
Albuquerque, NM 87185-0840

Abstract

A method is described for applying a sequence of peridynamic models with different length scales concurrently to subregions of a body. The method allows the smallest length scale, and therefore greatest spatial resolution, to be focused on evolving defects such as cracks. The peridynamic horizon in each of the models is half of that of the next model in the sequence. The boundary conditions on each model are provided by the solution predicted by the model above it. Material property characterization for each model is derived by coarse-graining the more detailed resolution in the model below it. Implementation of the multiscale method in the PDMS code is described. Examples of crack growth modeling illustrate the ability of the method to reproduce the main features of crack growth seen in a model with uniformly small resolution. Comparison of the multiscale model results with XFEM and cohesive elements is also given for a crack growth problem.

Acknowledgments

This work was sponsored by the Joint DOD/DoE Munitions Technology Program at Sandia National Laboratories.

Contents

Figures

1 Introduction

The peridynamic theory of solid mechanics [1, 2] is designed to unify the mathematical and computational modeling of continuous media, crack growth, and discrete particles. It accomplishes this by using integro-differential equations, rather than partial differential equations, as the basic mathematical tools. The integro-differential equations do not require the evaluation of spatial derivatives of the deformation or of a stress field. Hence, they are applicable even when the deformation contains discontinuities such as cracks. Using generalized functions, the same peridynamic equations also apply to systems of discrete particles, including molecular dynamics.

In the peridynamic theory, the equation of motion is given by

$$\rho(\mathbf{x})\ddot{\mathbf{u}}(\mathbf{x},t) = \int_{\mathcal{H}_\mathbf{x}} \mathbf{f}(\mathbf{q},\mathbf{x},t)\, dV_\mathbf{q} + \mathbf{b}(\mathbf{x},t) \tag{1}$$

where ρ is the density field, $\mathbf{u}$ is the displacement field, $\mathbf{x}$ is any material point in the body $\mathcal{B}$, $\mathbf{b}$ is a prescribed body force density field, and t is time. $\mathcal{H}_\mathbf{x}$ is a neighborhood of $\mathbf{x}$ called the *family* of $\mathbf{x}$. The radius of $\mathcal{H}_\mathbf{x}$ is called the *horizon*, denoted by δ. The function $\mathbf{f}$ is the *pairwise bond force density* field and has dimensions of force/volume^2. The integral in (1) sums up the force on $\mathbf{x}$ due to interactions with each material point $\mathbf{q}$ within its family (Figure 1).

The values of $\mathbf{f}$ are determined by the deformation and the material model. These values include contributions from the material model at both $\mathbf{x}$ and $\mathbf{q}$:

$$\mathbf{f}(\mathbf{q},\mathbf{x},t) = \mathbf{t}(\mathbf{q},\mathbf{x},t) - \mathbf{t}(\mathbf{x},\mathbf{q},t)$$

where each term on the right hand side represents a *bond force density* from the material model at $\mathbf{x}$ and $\mathbf{q}$ respectively. These bond forces are related to the deformation of the families of each point:

$$\mathbf{t}(\mathbf{q},\mathbf{x},t) = \underline{\mathbf{T}}(\underline{\mathbf{Y}}[\mathbf{x},t])\langle\mathbf{q}-\mathbf{x}\rangle, \qquad \mathbf{t}(\mathbf{x},\mathbf{q},t) = \underline{\mathbf{T}}(\underline{\mathbf{Y}}[\mathbf{q},t])\langle\mathbf{x}-\mathbf{q}\rangle$$

where $\underline{\mathbf{Y}}[\mathbf{x},t]$ and $\underline{\mathbf{Y}}[\mathbf{q},t]$ represent the deformations of $\mathcal{H}_\mathbf{x}$ and $\mathcal{H}_\mathbf{q}$ respectively. The vector $\mathbf{q}-\mathbf{x}$ is called the *bond* from $\mathbf{x}$ to $\mathbf{q}$. The values of each $\mathbf{t}$ therefore depend on the bond.

The abstract relations described above allow for very general material modeling. The force density $\mathbf{t}$ in each bond is determined not only by the deformation of that particular bond, but also by all the other bonds in its family. To allow this generality is the purpose of the abstract representation of peridynamic material models described above. The functions $\underline{\mathbf{Y}}$ and $\underline{\mathbf{T}}$ are examples of *peridynamic states*, which are simply vector-valued mappings defined on families.

A great simplification is achieved by giving up some of this generality, and assuming that each bond force density depends only on the deformation of that particular bond.

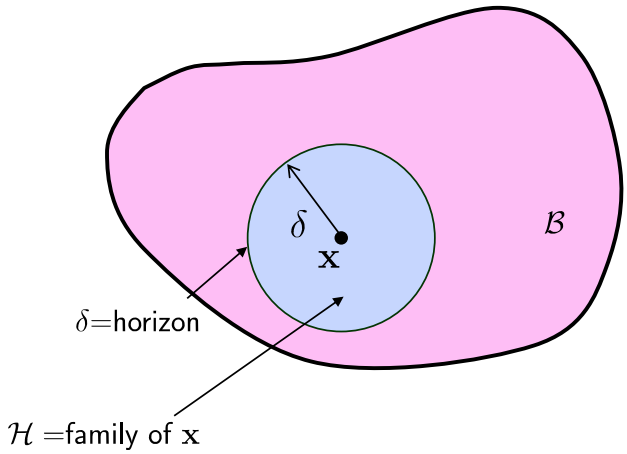

Figure 1. Family of a material point $\mathbf{x}$.

This restriction of the general theory is called *bond-based* peridynamics. In bond-based peridynamics, the equation of motion and material model simplify to

$$\rho(\mathbf{x})\ddot{\mathbf{u}}(\mathbf{x},t) = \int_{\mathcal{H}_\mathbf{x}} \mathbf{f}(\boldsymbol{\eta},\boldsymbol{\xi})\, dV_{\boldsymbol{\xi}} + \mathbf{b}(\mathbf{x},t) \tag{2}$$

where the bond and the relative displacement vector at its endpoints are given by

$$\boldsymbol{\xi} = \mathbf{q} - \mathbf{x}, \qquad \boldsymbol{\eta} = \mathbf{u}(\mathbf{q},t) - \mathbf{u}(\mathbf{x},t).$$

A further simplification results from assuming that a bond-based material model is linearly elastic. In this case, we can write

$$\mathbf{f} = c(\boldsymbol{\xi}) s \mathbf{M}, \qquad s = \frac{|\boldsymbol{\xi}+\boldsymbol{\eta}|}{|\boldsymbol{\xi}|} - 1, \qquad \mathbf{M} = \frac{\boldsymbol{\xi}+\boldsymbol{\eta}}{|\boldsymbol{\xi}+\boldsymbol{\eta}|},$$

where s is the *bond strain* (change in bond length divided by its initial length), and $\mathbf{M}$ is the deformed bond direction unit vector.

Damage can be incorporated into a bond-based peridynamic model using the idea of bond breakage. When a bond's deformation reaches some critical condition, the bond breaks irreversibly, meaning that it no longer carries any load. One way of expressing this is through a history-dependent bond damage variable μ that changes irreversibly from 1 to 0 at the time of bond breakage:

$$c(\boldsymbol{\xi}, t) = c_0(\boldsymbol{\xi})\mu(\boldsymbol{\xi}, t), \tag{3}$$

where c_0 is the undamaged spring constant. In the special case of constant c_0 independent of $\boldsymbol{\xi}$ (that is, constant within the family), the calibration of the model for three-dimensional formulations [3] leads to

$$c_0 = \frac{18k}{\pi\delta^4}. \tag{4}$$

The resulting bond-based material model is called the *prototype elastic brittle* (PMB) model. Although many bond damage laws are possible, the most widely used is based on critical bond strain:

$$s(\boldsymbol{\xi}, t_*) > s_* \qquad \Longrightarrow \qquad \mu(\boldsymbol{\xi}, t) = 0 \quad \text{for all } t \geq t_* \tag{5}$$

where s_* is a prescribed critical bond breakage strain and t_* is the time of bond breakage (usually not known in advance of modeling an application).

The horizon δ represents the maximum interaction distance for material points. Points $\mathbf{x}$ and $\mathbf{q}$ that are separated by an initial distance greater than δ do not interact, and are therefore excluded from the volume of integration $\mathcal{H}_\mathbf{x}$ in the equation of motion. When the scale of the modeling resolves the materials structure, the horizon is treated like a material property – a length scale correlated with the underlying material structure. When the scale of the modeling represents the material as a homogenous continuum, the horizon is a numerical parameter that is frequently chosen as a matter of convenience, since a peridynamic material model can usually be fitted to measurable material properties for any given value of δ.

Because the peridynamic equation of motion involves a volume integral over the family of each point, rather than local values of spatial derivatives of a stress field, boundary conditions are treated differently than in the standard theory of solid mechanics. Instead of prescribing displacement on the boundary, as in the standard theory, displacement must be prescribed in a layer with finite volume underneath the surface (Figure 2). This *boundary region* (more properly called a *constrained volume*) containing prescribed displacements is denoted $\mathcal{R}$, with $\mathcal{R} \subset \mathcal{B}$. The prescribed displacement field within $\mathcal{R}$ is denoted $\mathbf{w}$. Thus, a boundary-initial value problem with prescribed displacements for the PMB material model is defined by

$$\rho(\mathbf{x})\ddot{\mathbf{u}}(\mathbf{x}, t) = \int_{\mathcal{H}_\mathbf{x}} cs(\boldsymbol{\xi}, t)\mathbf{M}\, dV_{\boldsymbol{\xi}} + \mathbf{b}(\mathbf{x}, t), \qquad \mathbf{x} \in \mathcal{B} - \mathcal{R}, \;\; t \geq 0,$$

$$\mathbf{u}(\mathbf{x}, t) = \mathbf{w}(\mathbf{x}, t), \qquad \mathbf{x} \in \mathcal{R}, \;\; t \geq 0,$$

$$\mathbf{u}(\mathbf{x}, 0) = \mathbf{u}_0(\mathbf{x}), \qquad \dot{\mathbf{u}}(\mathbf{x}, 0) = \mathbf{v}_0(\mathbf{x}),$$

where $\mathbf{w}$, $\mathbf{u}_0$, and $\mathbf{v}_0$ are given functions.

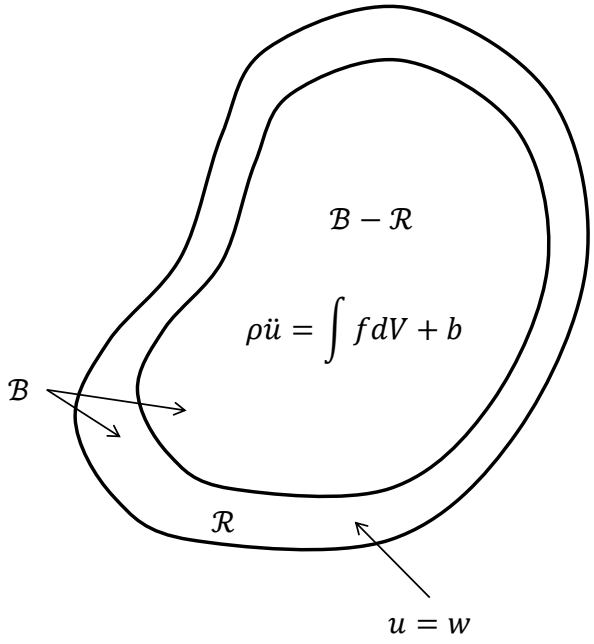

Figure 2. Boundary conditions (volume constraints) are applied to a peridynamic body $\mathcal{B}$ in a subregion of finite volume $\mathcal{R}$.

2 Multiscale method

Any application of peridynamics involves a choice of the horizon δ. Unlike more typical nonlocal models, the length parameter (the horizon in the case of peridynamics) influences the region of integration $\mathcal{H}_{\mathbf{x}}$ in the equation of motion and the material model. This raises the possibility that by varying δ, a multiscale method could be obtained. It is this possibility that motivates the method development described in the remainder of this report.

It would be convenient if δ could be prescribed arbitrarily as a function of position and time within a mathematical model of a body, allowing the smallest length scale to be applied in the vicinity of small features of interest such as crack tips or other defects. Unfortunately, non-constant values of $\delta(\mathbf{x}, t)$ result in undesirable artifacts in the predicted displacement field except in a few special cases.

Therefore, we pursue a different strategy for multiscale peridynamics. In this approach, a sequence of $L+1$ distinct models called *levels* is applied to different subregions of the body. Each level, which occupies the subregion $\mathcal{B}^\ell$, has a distinct but constant value of horizon denoted δ^ℓ, $\ell = 0, 1, \ldots, L$. The level 0 model provides the most detailed resolution and is assumed to contain the "best physics" at the smallest applicable length scale. Successive levels become progressively more smeared and continuum-like by applying larger length scales, and it is assumed that

$$\delta^0 < \delta^1 < \cdots < \delta^L.$$

Each level is a subset of the level above it:

$$\mathcal{B}^0 \subset \mathcal{B}^1 \subset \cdots \subset \mathcal{B}^L.$$

(Figure 3.) The highest level is identical to the full body:

$$\mathcal{B}^L = \mathcal{B}.$$

Let $\mathbf{u}^\ell$ denote the displacement field in level ℓ. All the levels obey the global initial conditions. Global body force densities are also applied identically in all levels.

Displacement boundary conditions on each level $\ell < L$ are derived from the level above it:

$$\mathbf{u}^\ell = \mathbf{u}^{\ell+1} \ \text{ on } \ \mathcal{R}^\ell \subset \mathcal{B}^{\ell+1}.$$

In other words, the boundary displacements in level ℓ are identical to whatever displacements are computed in the level above it. In summary, the levels obey a coupled set of initial boundary value problems:

$$\rho(\mathbf{x})\ddot{\mathbf{u}}^\ell(\mathbf{x}, t) = \int_{\mathcal{H}_{\mathbf{x}}{}^\ell} c^\ell s^\ell(\boldsymbol{\xi}, t)\mathbf{M}\, dV_{\boldsymbol{\xi}} + \mathbf{b}(\mathbf{x}, t), \qquad \mathbf{x} \in \mathcal{B}^\ell - \mathcal{R}^\ell, \ \ t \geq 0,$$

$$\mathbf{u}^\ell(\mathbf{x}, t) = \mathbf{u}^{\ell+1}(\mathbf{x}, t), \qquad \mathbf{x} \in \mathcal{R}^\ell, \ \ t \geq 0,$$

$$\mathbf{u}^\ell(\mathbf{x}, 0) = \mathbf{u}_0(\mathbf{x}), \qquad \dot{\mathbf{u}}^\ell(\mathbf{x}, 0) = \mathbf{v}_0(\mathbf{x}).$$

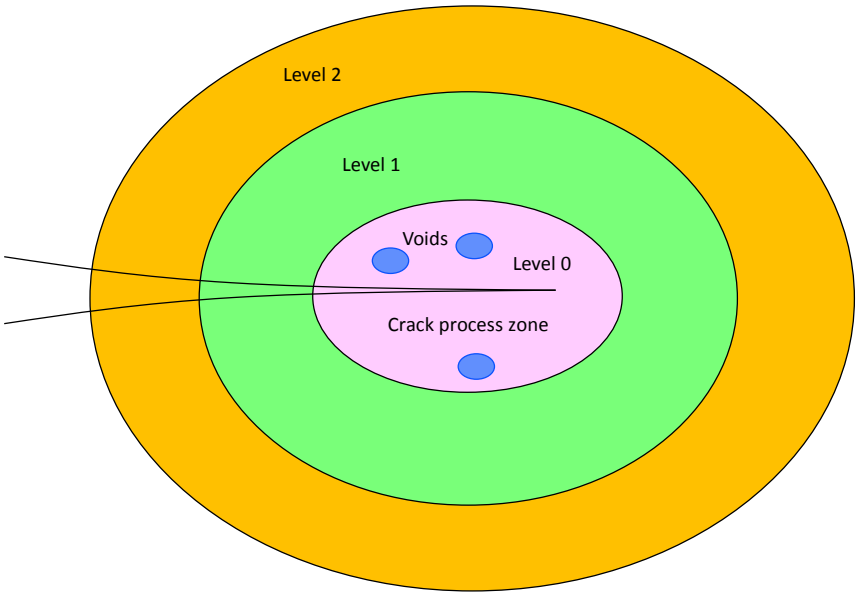

Figure 3. Levels surrounding a crack tip process zone.

Here, the family ${\mathcal{H}_{\mathbf{x}}}^{\ell}$ has horizon δ^ℓ. The spring constant c^ℓ is obtained using the same scaling law as in (4):

$$c^\ell(\boldsymbol{\xi}, t) = c_0^\ell(\boldsymbol{\xi})\mu^\ell(\boldsymbol{\xi}, t),$$
$$c_0^\ell = \frac{18k}{\pi(\delta^\ell)^4}. \tag{6}$$

Bond damage is mapped from level $\ell < L$ to the level above it by scaling the bond lengths. The damage variable μ^0 is "actively" computed from the deformation according to (5):

$$s^0(\boldsymbol{\xi}, t_*) > s_* \qquad \Longrightarrow \qquad \mu^0(\boldsymbol{\xi}, t) = 0 \quad \text{for all } t \geq t_*.$$

Higher levels have their bond damage determined not by their own deformation, but by coarse graining damage from the levels immediately below:

$$\mu^{\ell+1}(\boldsymbol{\xi}, t) = \mu^\ell\left(\frac{\delta^\ell}{\delta^{\ell+1}}\boldsymbol{\xi}, t\right), \qquad \ell = 0, 1, \ldots, L.$$

In summary, the general outline of the hierarchical multiscale method is as follows:

- Each level solves its own equation of motion.
- The boundary condition on each level comes from the solution at the level above it. (Exception: level L obeys only the global boundary condition.)

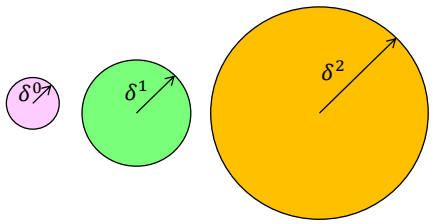

Figure 4. Higher levels have larger horizons.

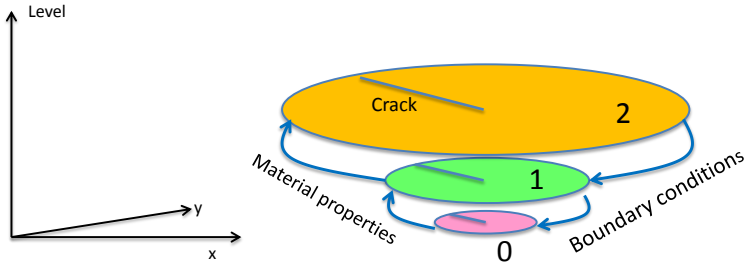

Figure 5. Schematic of interactions between levels.

- The damage at each level is coarse-grained up from the level below it. (Exception: damage in level 0 is determined by the deformation and material damage law.)

3 Numerical implementation

Sandia's PDMS ("PeriDynamic MultiScale") code solves the concurrent, hierarchical multiscale system described in the preceding section. In each level, it uses the discretization described in [3]. In this numerical method, the integral in (1) colorblue(in the absence of body loads) is evaluated using midpoint quadrature in a meshless discretization of the body:

$$\rho\ddot{\mathbf{u}}_i = \sum_{j\in\mathcal{H}_i} c_i s_{i,j}\mathbf{M}_{i,j}\Delta V_j$$

where i and j are node numbers, ΔV_j is the volume associated with node j, and $s_{i,j}$ is the bond strain in the bond from node i to node j:

$$s_{i,j} = \frac{(\mathbf{x}_j + \mathbf{u}_j) - (\mathbf{x}_i + \mathbf{u}_i)}{|\mathbf{x}_j - \mathbf{x}_i|} - 1.$$

The acceleration at node i is approximated with a central difference formula:

$$\ddot{\mathbf{u}}_i = \frac{\mathbf{u}_i{}^+ - 2\mathbf{u}_i + \mathbf{u}_i{}^-}{\Delta t^2}$$

where Δt is the time step size and $\mathbf{u}_i{}^-$ and $\mathbf{u}_i{}^+$ denote the values at the previous and next time steps respectively. As discussed in [3], a stability restriction applies to the time step size. This restriction can be expressed in the form

$$\Delta t \le \alpha\delta \tag{7}$$

where α is a constant, independent of δ, that is proportional to the wave speed of the material. Thus, the stability restriction is similar to the Courant-Friedrichs-Levy condition, with horizon playing the role of mesh spacing. The current method is "meshless" in the sense that there are no geometrical connections, such as finite elements, that connect the nodes.

In PDMS, each level $\mathcal{B}^\ell$ is represented by its own numerical grid. The region of space occupied by this grid changes with time, as $\mathcal{B}^\ell$ evolves. Each level has a horizon that differs from neighboring levels by a factor of 2:

$$\delta^\ell = 2^\ell\delta^0.$$

This exponential increase in horizon permits δ^ℓ to be used as a parameter that adaptively controls the mesh discretization. For example, higher levels could be applied away from some critical region such as a crack tip. Within these higher levels, a coarse discretization would provide sufficient accuracy to compute the nonlocal interactions with the larger value of δ^ℓ that is present there. The grids generated by PDMS occupy a cubic lattice with grid spacing in each level a factor of 2 greater than the one below it:

$$\Delta x^\ell = 2^\ell\Delta x^0.$$

Thus, the families in all levels contain the same number of nodes. The coupling between levels through boundary conditions and coarse-graining of damage is the same as described in the previous section.

Since the grid spacing differs by a factor of 2 between levels, the stability restriction (7) dictates that the time step also differ:

$$\Delta t^\ell = 2^\ell \Delta t^0.$$

Let the displacements at the start of a level L time step be denoted $\mathbf{u}^L(n)$. In each time step, the level L velocities and displacements are computed for the next time step, resulting in values for $\mathbf{u}^L(n+1)$. The boundary conditions in level $L-1$ are applied by applying linear interpolation to the level L displacements. Thus, in $\mathcal{R}^{L-1}$,

$$\mathbf{u}^{L-1}(n) = \mathbf{u}^L(n),$$

$$\mathbf{u}^{L-1}(n+1/2) = (\mathbf{u}^L(n) + \mathbf{u}^L(n+1))/2,$$

$$\mathbf{u}^{L-1}(n+1) = \mathbf{u}^L(n+1).$$

A similar interpolation determines the boundary conditions in each lower level from the solution in the level above it.

4 Node creation and deletion

As a crack grows, the process zone where a high level of resolution is needed moves with the crack tip. Therefore, PDMS redefines the level 0 subregion, along with the higher level regions up to $L-1$, as a function of time. To define $\mathcal{B}^0$ at any given time, it is first necessary to identify where the crack tip is located. There are three methods available in PDMS for doing this:

- Assume that the crack tip is located where damage is currently increasing. This method suffers from the limitation that it works for growing cracks but not static cracks (which might start growing due to subsequent loading).
- Assume that the crack tip is located where bond strains are comparable to the prescribed critical bond strain for the material. This method does not become effective until a crack is on the verge of growing. It also suffers from "false positives," that is, locations where there are large bond strains that never turn into growing cracks.
- Define through user input the locations where high resolution is needed. This method is effective near strong boundary loading, such as the impact point of a projectile against a target, but it is not useful for growing cracks whose location is not known in advance.

All of these methods can be used with PDMS, but none are completely general.

Once the location of a crack tip or other growing defect is identified at a given time t, the level 0 region $\mathcal{B}^0$ is chosen to extend a fixed distance from this location. This distance is typically chosen to be $5\delta^0$. Of this $\mathcal{B}^0$, the outer layer of thickness δ^0 comprises the boundary region $\mathcal{R}^0$. As discussed in the previous sections, displacements within this boundary region are taken from the solution in the next higher level, $\ell = 1$. At all other points in $\mathcal{B}^0$, the level 0 equation of motion is applied to find $\mathbf{u}^0$ as a function of time.

As the crack tip moves, level 0 nodes are created according to the current definition of $\mathcal{B}^0$. Level 0 nodes are also deleted as the subregion moves away from them.

Higher levels are defined similarly based on the current geometry of the level immediately below them. Level 1 is defined to include all of level 0 as well as material out to an additional distance $5\delta^1$. Thus, as $\mathcal{B}^0$ changes, $\mathcal{B}^1$ and all higher levels up to $\ell = L-1$ change with it. Note that the highest level never changes, since $\mathcal{B}^L = \mathcal{B}$ by definition.

5 Example

Consider the plate with a pre-existing edge crack shown in Figure 6. This compact tension type specimen was inspired by a recent problem for a ductile fracture modeling challenge [4]. While this specimen might more typically be used to measure the fracture energy of a material, here we focus on the crack propagation predicted by the method. Simplified displacement boundary conditions, applied to the lower edges, were substituted for the more complex pin connections of the actual specimen. Both boundary conditions produce an increasing crack opening displacement along the specimen's edge that causes the crack to grow. As with a double cantilever specimen, one would expect the crack path to be unstable. To compare PDMS model results with those of FE methods using cohesive zone and XFEM crack growth models, we only consider propagation of a straight crack. The FEM analyses constrain the crack to a straight path, while the PDMS simulations produce a straight crack path due to the model symmetry and homogeneity of the material parameters.

In the peridynamics formulation, we do not have an equivalency between the bond failure model and a corresponding cohesive zone representation. However, under the assumption made in linear elastic fracture mechanics (LEFM) of a small process zone, we expect the two formulations to approximate each other, because the results should depend upon the fracture energy alone and not upon the specific traction separation behavior. (In contrast, a "quasi-brittle" problem is characterized by a relatively large process zone for which the traction separation response can have a significant effect upon the specimen's response.)

In comparing the PDMS model with FE models, it should be noted that the two approaches approximate LEFM in different senses. To obtain results representative of LEFM for a cohesive crack model, one would typically hold the fracture energy constant while examining the predicted response for analyses with increasing strength (peak traction in the cohesive zone model). The corresponding critical crack opening would decrease with the increase of strength eventually yielding results where the size of the cohesive zone is sufficiently small to closely approximate LEFM. For the peridynamics analyses one could obtain results approaching those of LEFM by reducing the size of the level 0 horizon. In this example problem, the "limiting studies" that one could conduct with the different computational methods to approach LEFM are not addressed, so we only anticipate that the results will be qualitatively close but not as close as the two FEM results (both of which use cohesive zone models).

For a brittle fracture model problem, we assume properties representative of a soda-lime-silicate glass. The assumed fracture energy is 6.5 J/m^2, and for the FEM models used in comparison [5] we start with a strength of 27 MPa, which is toward the low end of nominal strengths for the material. In the FEM results the size of the cohesive zone remained close to 0.5 mm during the crack propagation [5]. This length was about 10 percent of the original crack length and thus about 5 percent of the crack length by the time it had grown another 5 mm. Figure 7 depicts the simulated growth of the crack with the PDMS formulation, showing both the bond strains and damage process zone.

Figure 8 shows computational results for boundary load as a function of boundary displacement. As shown in the figure, essentially the same results are obtained for multiscale PDMS simulations with $L = 0$ (fine resolution throughout) and with $L = 1$ or 2. Also, as noted in the figure, the multiscale model with $L = 2$ results in significant reduction in computation time, provided a sufficiently large geometry is modeled. For smaller models, the overhead required to perform the communications between multiscale levels tends to outweigh the savings in reducing the total number of nodes.

Figure 9 compares the peridynamic results with finite element results using XFEM and cohesive (interface) elements. The two finite element curves agree with each other very closely, principally because both formualtions use the same cohesive zone model to represent the crack surface evolution. The two peridynamic curves are both obtained with the PDMS code with slightly different definitions of the boundary regions. The peridynamic results are for $L = 0$ (that is, without the multiscale capability available in PDMS). Differences of about 10% are evident between the peridynamic and finite element results. However, it is not possible to determine which of these results are more accurate, since an exact solution is not available and (as previsouly noted) complete parameter studies to make each formulation approach LEFM have not been conducted. Figure 10 shows a limited convergence study where the size of the horizon is scaled down with grid refinements. The peridynamic results for the finest grid and smallest horizon differ the least with the finite element results.

Figure 11 illustrates a similar demonstration problem at a higher rate of loading using PDMS with $L = 2$. In this problem, the crack grows dynamically and branches. The predicted crack growth velocities are found to be admissible physically, that is, less than the Rayleigh wave speed.

Crack branching can also occur due to heterogeneity of a material, as illustrated in Figure 12. In this PDMS simulation with $L = 2$, an edge crack grows into a medium with a dense distribution of hard inclusions. This type of phenomenon may be related to the observed diffusion or smearing of cracks in heterogeneous materials such as concrete and other composites.

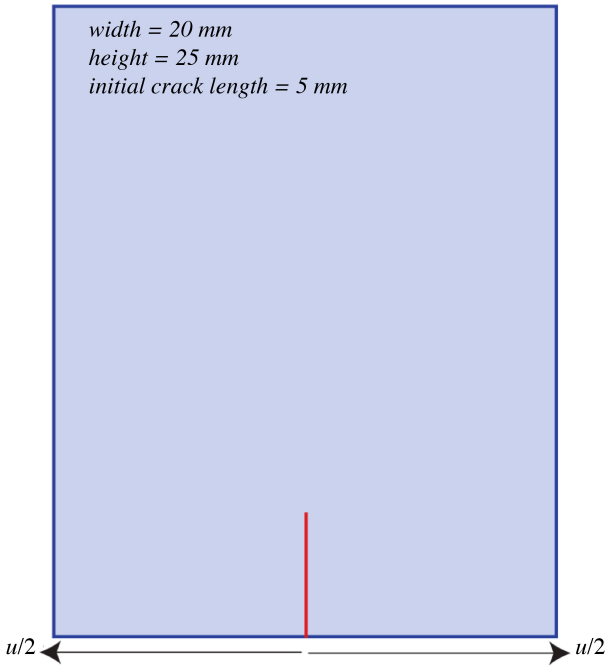

Figure 6. Compact tension specimen with a 5 mm pre-existing edge crack. This schematic of the model does not include extensions of the domain on the bottom to apply displacement boundary conditions to the PDMS model.

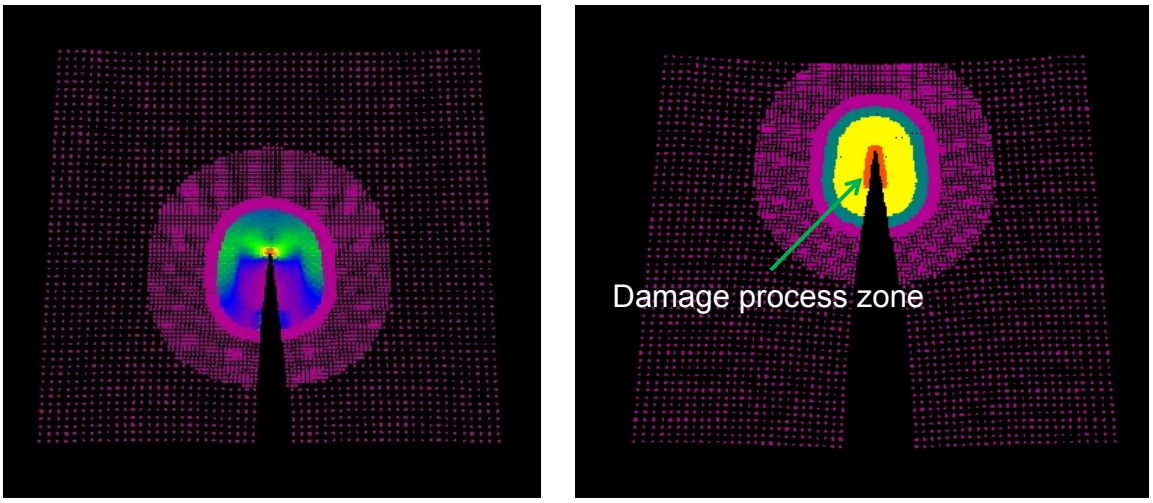

Figure 7. Simulated growth of an edge crack. Left: colors indicate bond strain. Right: crack process zone and surrounding higher-level subregions.

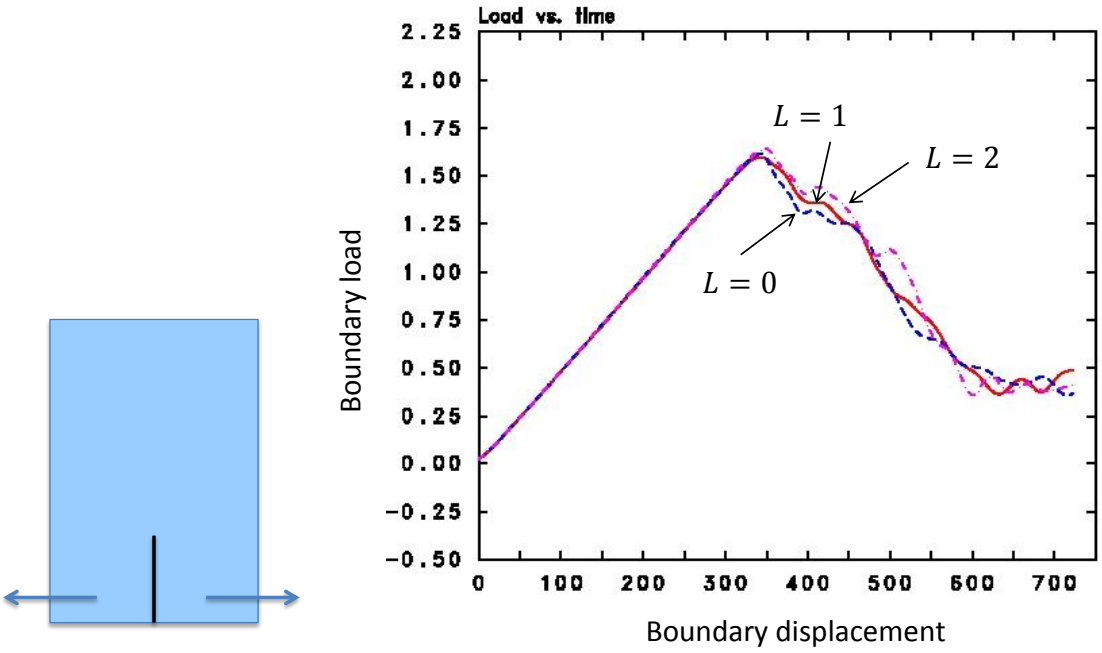

Level	Wall clock time (min) with 28K nodes in coarse grid	Wall clock time (min) with 110K nodes in coarse grid
0	30	168
2	8	16

Figure 8. Comparison of predictions for the edge crack growth problem using different numbers multiscale levels.

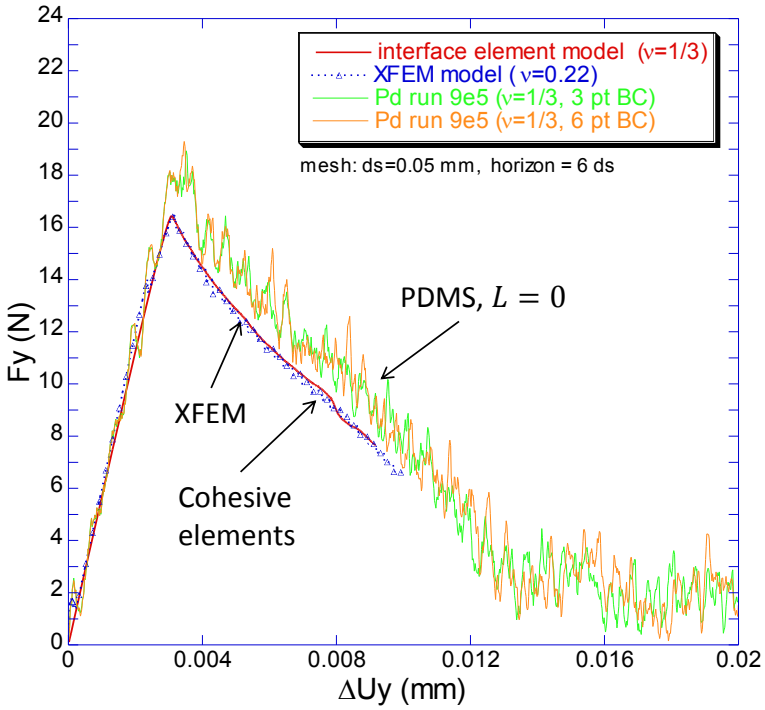

Figure 9. Comparison of predictions for growth of an edge crack in a brittle plate using PDMS and finite elements. The two PDMS results show the minor effect of changing the size of the boundary region.

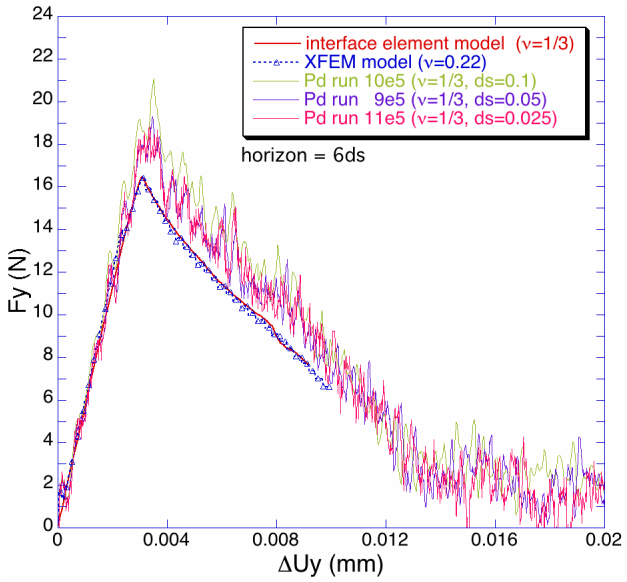

Figure 10. Comparison of predictions for growth of an edge crack in a brittle plate using PDMS and finite elements. The three PDMS results show the minor effect of changing the size of the grid and the grid-scaled horizon.

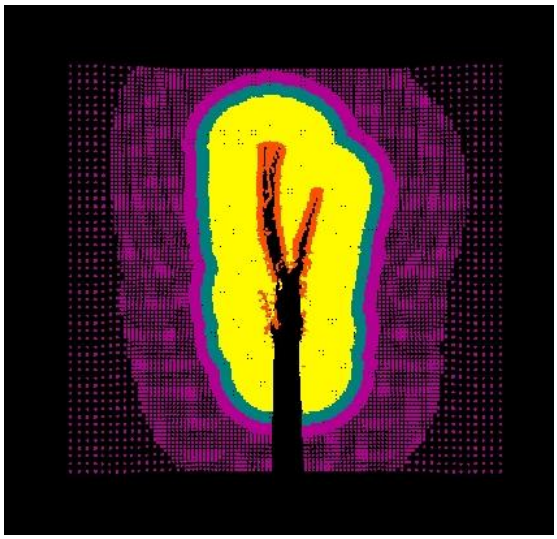

Figure 11. High-rate loading of a plate with an edge crack results in crack branching.

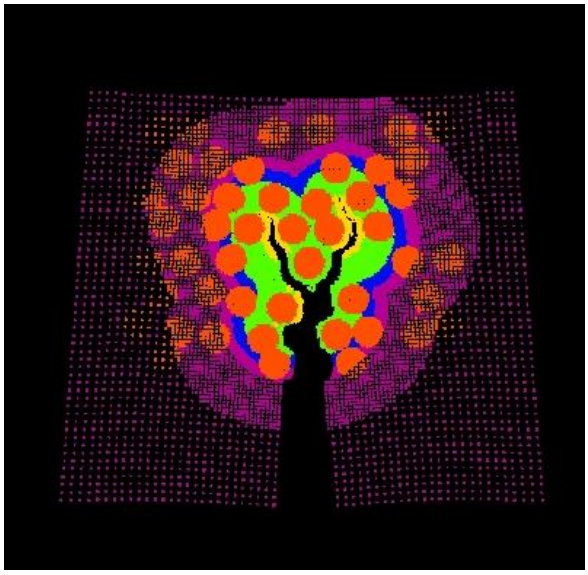

Figure 12. Crack branching in a heterogeneous medium with hard inclusions.

6 Discussion

The multiscale approach discussed in this report has the following advantages:

- The same equations are used at each level; only the value of the horizon changes.
- Levels interact only with the level immediately above and below.
- Each level solves only its own equation of motion. This is important because it avoids the difficulty of solving all the levels simultaneously.
- Each level uses its own time step. Higher levels use larger time steps than lower levels. In this sense, the method is multiscale in time as well as space.
- Small scale phenomena such as crack tip process zones can interact with larger scale structural response. The computational cost of increasing the size of a structure being modeled is small, provided that most of it is in level L (thereby requiring only the coarsest discretization.

The method has the disadvantage of involving computational complexity in programming the communications between levels, but this is perhaps true of all available multiscale techniques. Another disadvantage is that if there are many cracks that are widely distributed throughout a structure, the multiscale method treats nearly the whole body as level 0, negating any savings in computational cost.

References

[1] S. A. Silling, Reformulation of elasticity theory for discontinuities and long-range forces, *Journal of the Mechanics and Physics of Solids* **48** (2000) 175–209.

[2] S. A. Silling and R. B. Lehoucq, Peridynamic theory of solid mechanics, *Advances in Applied Mechanics* **44** (2010) 73–168.

[3] S. A. Silling and E. Askari, A meshfree method based on the peridynamic model of solid mechanics, *Computers and Structures* **83** (2005) 1526–1535.

[4] B. L. Boyce, J. E. Bishop, A. Brown, T. Cordova, J.V. Cox, T.B. Crenshaw, K. Dion, J.M. Emery, J. T. Foster, J W. Foulk III, D. J. Littlewood, A. Mota, J. Ostien, S. Silling, B. W. Spencer, G. W. Wellman, Ductile failure X-prize, Sandia Report SAND2011-6801 (2011).

[5] J. V. Cox, Selected preliminary results for the application of analytically enriched XFEM to problems with small cohesive zones, Sandia Technical Memorandum (2011).

[6] J. V. Cox, An extended finite element method with analytical enrichment for cohesive crack modeling, *International Journal for Numerical Methods in Engineering* **78** (2009) 48-83.

DISTRIBUTION:

1 MS 0899 Technical Library, 9536 (electronic copy)

Sandia National Laboratories